Perylene π–Bridges that Equally Delocalize Anions and Cations. Quinoidal and Aromatic Contents in the Right Portion

Paula Mayorga Burrezo,[†,a] Wangdong Zeng,[‡,a] Michael Moos,[§] Marco Holzapfel,[§] Sofia Canola,[⊥] Fabrizia Negri,[⊥,*] Concepciò Rovira,[†] Jaume Veciana,[†] Hoa Phan,[‡] Jishan Wu,[‡,*] Christoph Lambert,[§] Juan Casado[*,∥]

[†]Department of Molecular Nanoscience and Organic Materials, Institut de Ciència de Materials de Barcelona (ICMAB)/CIBER-BBN, Campus Universitari de Bellaterra, E-08193, Cerdanyola, Barcelona, Spain

[‡]Department of Chemistry, National University of Singapore, 3 Science Drive 3, Singapore, 117543, Singapore

[§]Institut für Organische Chemie & Center for Nanosystems Chemistry, Julius-Maximilians-Universität Würzburg, 97074 Würzburg, Germany

[⊥]Dipartimento di Chimica 'G. Ciamician', Università di Bologna, Via F. Selmi 2, 40126/ INSTM, UdR Bologna, Italy

[∥]Department of Physical Chemistry, University of Malaga Campus de Teatinos s/n, 229071 Malaga, Spain

Supporting Information Placeholder

ABSTRACT: A complete study by electrochemistry, optical and EPR spectroscopies and quantum chemical calculations of aromatic and quinoidal perylene-based bridges, substituted either with bis(diarylamine) or with bis(arylimine) groups, has been carried out. The mixed valence properties of their radical cation and radical anion species have been analyzed in the framework of the Marcus-Hush theory, from which the through-bridge inter-redox site electronic couplings (V_{AB}) have been extracted. The unusual similitudes of the resulting V_{AB} values of the perylene based bridges, compared with other reported cases, reveal the intervention of molecular shapes with balanced semi-quinoidal/semi-aromatic structures in the charge delocalization. That an identical molecular object could equally respond to injection of positive or negative charges is rare in the field of organic π–conjugated molecules. We probe this in perylene based systems but can be extrapolated to others π–conjugated bridges and can open the door to the rational design of true ambipolar molecular conductors.

Organic mixed valence (MV)[1,2] molecules are key molecular models to test electron transfer theories in Chemistry, as well as for the conceptual design of new and more efficient wires for single molecular electronics.[3,4] The prototypical MV molecule is constituted by a conjugate bridge that connects two redox-active terminal groups, either oxidable donor groups or reducible acceptors. The MV property emerges in the monovalent redox species, either the radical cation or radical anion, due to the competition of the charge being localized on the one or the other redox center. The electron/hole transfer event over the bridge depends on several molecular factors, such as the nature of the redox-active groups or the bridge (i.e., length, conformation, composition, etc.) and of the surrounding medium, etc.[5,6] Regarding the terminal groups, if these are electron-acceptors, electrons are transferred in radical anions, while, if they are electron-donor groups, holes are transferred in radical cations. MV studies in molecular species with the same bridge and terminally substituted with donors or acceptors units have been thoroughly prepared and studied.[3-6,7,8,9,10,11,12] For ones and others, groups with different redox strength have been reported.

Remarkably, to the best of our knowledge, no studies of charge transfer –holes in radical cations and electrons in radical anions– have been carried out over the same bridge and between essentially the same terminal groups, such as highlighted in Scheme 1. This is a logical situation since organic redox-active groups usually are either donors (i.e., bad acceptors) or acceptors (i.e., bad donors) but not simultaneously good for both. Another aspect to consider, in order to afford the objective of analyzing the electron / hole charge delocalization regime within the same bridge & redox-groups architectures, is the fact that π–conjugated bridges themselves are typically electron donor moieties. Consequently, they become preferentially oxidized (than reduced) in redox studies. This means that, when combined with acceptors in the reduction processes, they are inherently resistive to electron delocalization. Hence, designing MV systems in which the capability of a same π–conjugated bridge with a similar behavior faced with electrons and holes (having all other factors almost equal, Scheme 1) is a current challenge.

Scheme 1 Radical cation and anion with identical bridges and very similar redox-active groups, $^{\bullet}G \approx {}^{\bullet}G'$ and $^{+}G \approx {}^{-}G'$.

To cope with this this task, dealing with inherently different starting neutral π–bridges, either aromatic or quinoidal compounds[13,14,15,16,17] (**1** and **2** in Scheme 2) has been the chosen approach. These structures are designed in such a way that upon oxidation of the first aromatic based compound (i.e., **1** → **1**$^{\bullet+}$ in Scheme 2) a partial quinoidization (or partial remaining aromatization) of the bridge is produced. Conversely, reduction of the second quinoidal based compound (i.e., **2** → **2**$^{\bullet}$) affords the attainment of a partial aromatization (or remaining partial quinoidization), such as depicted in Scheme 2. In this way, similar bridge structures for the radical cation and anion species can be accounted for. Regarding the redox sites, bis(diarylamine) groups have been chosen as the electron donor groups to be attached to the neutral aromatic bridge. Its synthesis is described in Section 1 of the Supporting Information file (Scheme S1 and Figures S1-S8). On the other hand, the neutral quinoidal core in **2**, whose synthesis was already reported by some of us,[18] connects two bis(arylimine) groups. Such as shown in Scheme 2, similar characters on the two CN moieties are achieved after the oxidation of the aromatic bis(diarylamine) and reduction of the quinoidal bis(arylimine). Thus, the resulting redox-active groups, (i.e., half-amine or half-imine), either in the radical cation or anion, are alike. All in all, with the MV property study of **1** and **2**, analogous semi-amine (semi-imine) and semi-quinoidal (semi-aromatic) structures are obtained either for the delocalization of the charge through the perylene bridge. which will allow us to explore the desired properties above described. Then, having been linked to similar redox-active groups, the role of the perylene unit in the intramolecular charge transport will be mainly tested. A complete study, including electrochemistry and spectroelectrochemistry, electron paramagnetic resonance spectroscopy, as well as quantum chemical calculations, is reported.

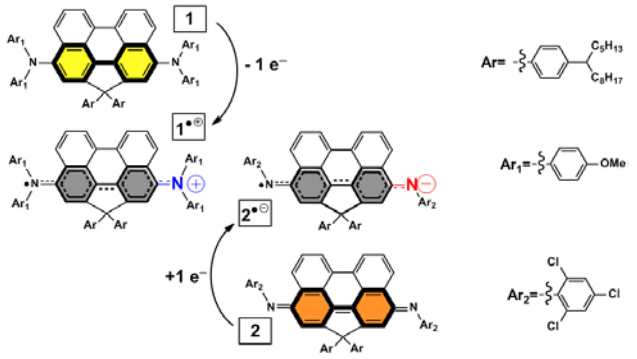

Scheme 2 Chemical structures of **1** and **2** and their MV radical cation (i.e., **1**$^{\bullet}$) and radical anion (i.e., **2**$^{\bullet}$) formed by oxidation and reduction, respectively.

Figure 1 depicts the electrochemical properties of **1** and **2**. Both of them display two reversible processes, anodic for **1** (Figure 1a) and cathodic for **2** (Figure 1b), leading to the consecutive generation of the radical cation (**1**$^{\bullet+}$) and dication in the first case, and of the radical anion (**2**$^{\bullet-}$) and dianion, in the second one. Similar separations between each two processes (0.19 V for **1** and 0.16 V for **2**, see Section 2 of ESI file, Table S1 and S2 and Figure S9-S12) should be highlighted. Considering the two monovalent species already delocalized (partially or totally) over the bridge, this energy should be associated with that required to localize the two charges, either positives or negatives, into the terminal groups (due to repulsion energy) in the divalent forms. Hence, comparable differences between the redox potentials of both samples can be considered as a first hint of a similar nature of the π-conjugated bridge after the removal or addition of a single electron.

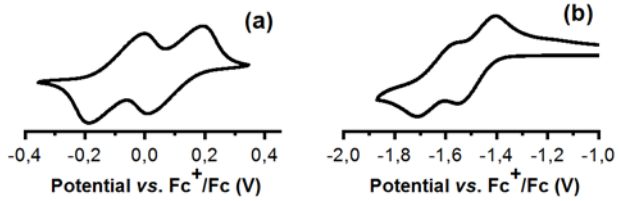

Figure 1. Cyclic voltammograms of **1** (a) and **2** (b) recorded at room temperature under Ar atmosphere (10^{-4} M/ 0.03 M TBA·PF_6/ *o*-DCB).

Encouraged by the reversibility and stability of the electrochemical processes, spectroelectrochemical UV-Vis-NIR absorption measurements were carried out for compounds **1**, under oxidation conditions, and **2**, under reduction ones (Figure 2a and 2c, respectively and Figures S13 and S14). Progressive disappearance of the 544 nm band during oxidation of **1** was observed, giving way to the rise of two new absorptions at 846 and 1446 nm through isosbestic points. Subsequent oxidation of **1**$^{\bullet+}$ yielded the dication, **1**$^{2+}$, which was characterized by one very strong band at 833 nm, completely dominating the UV-Vis-NIR absorption spectrum. This last feature is in good agreement with the appearance of a closed-shell quinoidal structures within the perylene unit between the two diarylamines in **1**$^{2+}$. Conversely, the reduction of **2** provoked the decrease of the band at 449 nm, accompanied by the increase, once again through isosbestic points, of the bands at 760 and 1238 nm, related to the radical anion species, **2**$^{\bullet-}$. Posterior reduction of **2**$^{\bullet-}$ gave way to the appearance of a new band at 747 nm together with the one at 441 nm, ascribed to the dianion, **2**$^{2-}$, after the full clearance of the bands discussed for the radical anion.

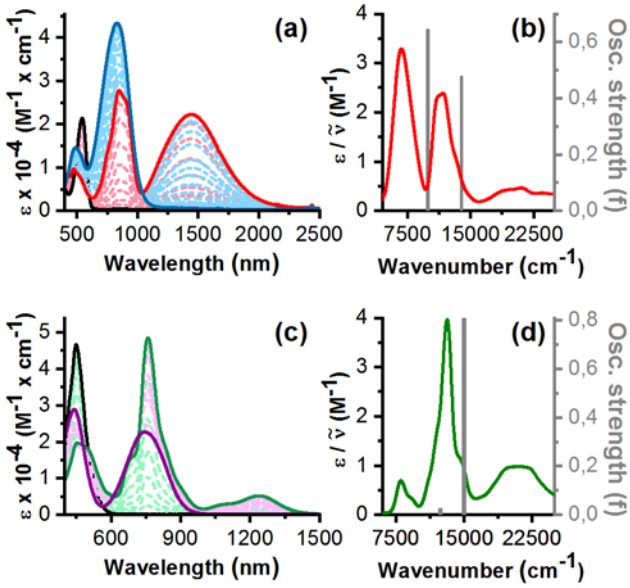

Figure 2. Electrochemically obtained (10^{-4} M/ 0.03M TBA·PF_6/ *o*-DCB) UV-Vis-NIR absorption spectra during oxidation of **1**: (a) neutral species, black solid line; radical cation, red solid line; dication, blue solid line, and reduction of **2**: (c), neutral species, black solid line; radical anion, green solid

line; dianion, purple solid line. Additionally, the absorption spectra of $\mathbf{1}^{\bullet+}$ (b) and $\mathbf{2}^{\bullet-}$ (d) have also been included with their respective results from TD-UBLYP35/6-31G** calculations including *o*-DCB solvent described with PCM.

Figure 2 also shows the reduced ($\varepsilon/\tilde{\upsilon}$) absorption spectra of the two pure radical species, $\mathbf{1}^{\bullet+}$(b) and $\mathbf{2}^{\bullet-}$ (d), extracted from the spectroelectrochemical data. In both cases, a low-energy feature, that might be associated with the so-called intervalence charge transfer band (i.e., IV-CT band), was found. Aiming to corroborate this hypothesis, as well as the assumptions displayed in Scheme 2, DFT geometry optimizations of the neutral and charged species were carried out and TD-DFT calculations were performed for the two systems (see Section 4 of ESI file, Figures S15, S16 and S17). As depicted in Figure 2 (b) and (d), a good experiment versus theory matching was obtained. As expected, the dominant nature of the lowest excited state, this is HOMO-1→HOMO for $1^{\bullet+}$ and LUMO→LUMO+1 for $2^{\bullet}$, corroborated the assignment of the IV-CT band (see Figure 3 and Figure S18 and S19 and Table S4). Importantly, an equivalent contribution of both redox centers in each case was detected as clearly shown by the shape of the molecular orbitals shown in Figure 3. It is known that, in order to reach full delocalization among redox centers (i.e., a Robin–Day class III situation)[3], the V_{AB} must fulfill the 2 $V_{AB} > \lambda_{AB}$ condition, with λ_{AB} as the intramolecular reorganization energy. According to a two-level model, for a Robin-Day class III situation, V_{AB} between the two redox centers can be evaluated as one half of the excitation energy of the IV-CT band.[4,6] Therefore, the assessment of the Robin-Day class, to which $\mathbf{1}^{\bullet+}$ and $\mathbf{2}^{\bullet-}$ belong, became of fundamental importance. To this end, two approaches were adopted: first, we investigated the electronic communication between the bridge and the donor/acceptor groups by building an orbital interaction diagram (i.e., Figure 3). In this sense, each molecule was thought as the combination of two terminal donor or acceptor groups and a π-conjugated bridge represented by the perylene unit. Therefore, **1** was considered as a Donor-Bridge-Donor (DBD) system, while **2** responded to an Acceptor-Bridge-Acceptor (ABA) one. Accordingly, calculations were carried out on the full DBD or ABA molecules at its neutral optimized geometry and, separately, for the two fragments: the perylene fragment on one side and the dimer formed by two donor (or acceptor) groups, on the other side. As shown in Figure 3, a strong interaction occurred in **1** between the anti-symmetric combination of the two degenerate occupied orbitals of the two donor fragments and the HOMO orbital of the perylene fragment with a large contribution of the bridge to the HOMO and HOMO-2 of DBD. In the framework of an orbital interaction diagram, the energy splitting provides an estimate of twice the coupling between the donor and the bridge[19] which is accordingly very large and matches an expected Robin Day class III system.

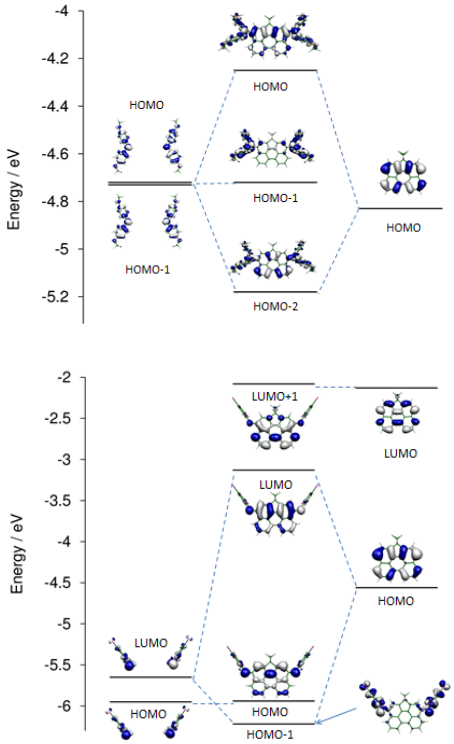

Figure 3 DFT//B3LYP/6-31G** orbital interaction diagrams for **1 (top)** and 2 (bottom) between the two fragments (perylene bridge on the right, and donor dimer or donor acceptor dimer on the left).

A second approach, based on the determination of the optimized geometries of $\mathbf{1}^{\bullet+}$ and $\mathbf{2}^{\bullet-}$, was used aiming at verifying the assignment. In both cases a delocalized distribution of the charge over the entire DBD or ABA system was revealed, in agreement with a class III. Indeed, Figure 3 shows that, in the case of $\mathbf{1}^{\bullet+}$, the initial state and the state created by the excitation from the HOMO-1 to the HOMO of DBD, determine the adiabatic + and – combination of the D^{+}-B-D and D-B-D^{+} localized diabatic states.[20] Thus, a correspondence of the HOMO-1→HOMO with the excitation into the IV-CT band was made. The V_{AB} was therefore estimated from the TD-UBLYP35 computed excitation energies (Tables S4 and S5) of the IV-CT transition, resulting to be 4315 cm^{-1}. Same procedure was followed for **2** (Figure 3) whose orbital interaction diagram demonstrates a large electronic communication between the bridge and the acceptors. In this case, an interaction between the HOMO of perylene fragment and the antisymmetric combination of the unoccupied acceptor's orbitals occurs. The flow of electrons from the perylene HOMO to the acceptor's orbitals, ultimately determines the quinoidal structure of the former in the neutral state. Analogously to the DBD system, in $\mathbf{2}^{\bullet-}$, one-electron excitation from the LUMO to the LUMO+1 corresponds to the excitation into the IV-CT. The V_{AB} between the two redox centers, obtained with the same procedure as for **1**, amounts to ca. 5686 cm^{-1} (Table S4 and 5). Interestingly, $\mathbf{1}^{\bullet+}$is produced by extracting one electron from the its HOMO by which, given its aromatic nature, allows a reduction of the overall aromatic character in favor of a quinoidal gaining. Conversely, $\mathbf{2}^{\bullet-}$ is produced by adding one electron into its LUMO which is also of aromatic nature by which the molecule gains a partial aromatic character in detriment of the quinoidal.

Thus, both ions acquire a partial aromatic shape which turns out to be similar in extent.

Comparing the theoretical V_{AB} and λ_{AB} values evaluated for the redox centers of $\mathbf{1}^{\bullet+}$ and $\mathbf{2}^{\bullet-}$, λ_{AB} never exceeds 2500 cm^{-1} (Table S5), corroborating the class III MV assignment in both cases. Experimental V_{AB} values were also determined considering the energy of the IV-CT band (i.e., $\bar{\upsilon}_{max}$) from the UV-Vis-NIR spectra, by using $2V_{AB} = \bar{\upsilon}_{max}$. Asymmetric shapes of these IV-CT bands, typical of Class III MV behavior, were supported by double-peak fitting in $\mathbf{1}^{\bullet+}$ and $\mathbf{2}^{\bullet-}$ (Section 5 of ESI file, Figures S20 and S21 and Tables S6 and S7). As a result, V_{AB} was set to 3464 cm^{-1} for $\mathbf{1}^{\bullet+}$ ($\bar{\upsilon}_{max}$ = 6928 cm^{-1}) and 4041 cm^{-1} for $\mathbf{2}^{\bullet-}$ ($\bar{\upsilon}_{max}$ = 8082 cm^{-1}) in good agreement with the theoretical values.

The generation of the class III MV species upon oxidation of **1**, given the energy proximity between the bridge HOMO orbital of the perylene and those of the donors (Figure 3) provokes the partial attainment of a quinoidal structure via emptying its HOMO orbital. According to calculations, in **2**, reduction of the arylimine groups is coupled to the bridge by interaction through their empty LUMO orbitals with the HOMO of the perylene moiety. Consequently, charging in $\mathbf{1}^{\bullet+}$ produces the partial rupture of the aromatic shape of the bridge rings, while that of the electron in $\mathbf{2}^{\bullet-}$ is supported by an underlying partial aromaticity recovery of the rings of the bridge. This means that oxidation of **1** and reduction of **2** mix these two geometrical configurations very much in the same proportion (i.e., see the comparison between the geometries of $\mathbf{1}^{\bullet+}$ and $\mathbf{2}^{\bullet-}$ in Figure S19). In addition, a diarylamino group acquires a partial imine character upon oxidation, while reduction of the arylimine group induces an equivalent loss of its intrinsic character. The overall outcome is the adoption of very similar shapes in $\mathbf{1}^{\bullet+}$ and in $\mathbf{2}^{\bullet-}$, what translates into similar charge delocalization properties.

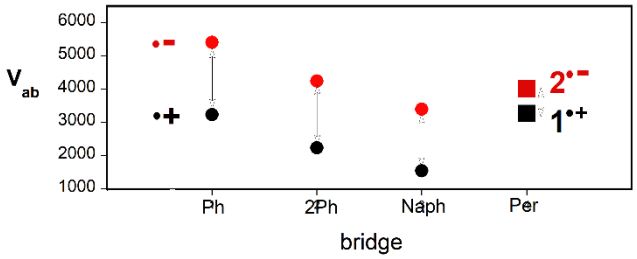

Figure 4. As filled circles: representation of the experimental V_{AB} for class III MV radical cations derived from bis(arylamino)phenylene (Ph), bis(arylamino)biphenyl (2Ph) and bis(arylamino)naphthylene (Naph). As red circles: representation of the V_{AB} for class III MV radical anions derived from bis(nitroaryl)phenylene (Ph), bis(nitroaryl)biphenyl (2Ph) and bis(nitroaryl)naphthylene (Naph). As filled black and red squares are the values for $\mathbf{1}^{\bullet+}$ and $\mathbf{2}^{\bullet-}$, respectively.

These certainly large V_{AB} values of $\mathbf{1}^{\bullet+}$ and $\mathbf{2}^{\bullet-}$, particularly that for $\mathbf{1}^{\bullet+}$, resulted to be among the largest found in the literature for bis(diarylamino) phenyl based compounds. For instance, it is similar to that of bis(diarylamino) substituted benzene (benzene as a bridge, V_{AB} = 3240 cm^{-1}),[21] larger than that with a naphthalene bridge[21] (V_{AB} = 2240 cm^{-1}) and more than twice the value in the case of the biphenyl bridge (V_{AB} = 1550 cm^{-1}).[21] Unfortunately, the repertory of V_{AB} for radical anions is much more limited in the literature than those of the radical cations. However, the following cases of V_{AB} values for bis(nitroaryl) funcionalized[22,23] series can be mentioned: i) for benzene as a bridge, V_{AB} = 5410 cm^{-1}, for bis(nitroaryl) biphenyl radical anion, V_{AB} = 3400 cm^{-1}, and for the analogue with a naphthalene bridge, V_{AB} = 4250 cm^{-1}. In this context, the V_{AB} value for $\mathbf{2}^{\bullet-}$ fits among the best obtained so far.[6] Figure 4 compiles the V_{AB} values of the above described compounds together with those reported in this work. The V_{AB} values for the radical anions are, in general, much larger than those of the radical cations (i.e., notice the different condition regarding solvent and counterions).[6,21,22,23] Nonetheless, these differences are strongly reduced in the case of $\mathbf{1}^{\bullet+}$ *vs* $\mathbf{2}^{\bullet-}$.

Longer π-conjugated bridges (i.e., quaterrylene and hexarylene units) with the same substitution pattern as **1** and **2** were also prepared (Scheme S1) and studied by electrochemistry (Figures S22 and S23 and Tables S8 and S9), UV-Vis-NIR spectroelectrochemistry (Figures S24, S27, S30 and S33) and quantum chemistry (Figures S25, S26, S28, S29, S31, S32, S34 and S35) and Figures S1-S8).. Unfortunately, none of them could be analyzed in the context of MV framework due to a higher relevance of the central connecting bridge: *(i)* considering the radical cations of these two bis(diarylamine) derivatives, the electron oxidation took place mostly on the central connecting bridge;[24] *(ii)* in the case of the radical anions of the bis(arylimine) series, a residual involvement of the arylimine groups in the charge exchange was detected. In order words, the negative charge was preferentially stabilized on the quinoidal bridge.

Finally, Figure 5 shows the experimental and simulated EPR spectra of $\mathbf{1}^{\bullet+}$ and $\mathbf{2}^{\bullet-}$ recorded at low temperature (200 K). $\mathbf{1}^{\bullet+}$ exhibits a five evenly spaced main lines[11,25] corresponding to the hyperfine coupling of the unpaired electron with two magnetically equivalent ^{14}N atoms with coupling constants of 0.32 mT. In the case of $\mathbf{2}^{\bullet-}$, seven lines were found associated with the previously mentioned coupling of the unpaired electron with two magnetically equivalent ^{14}N atoms (a_N = 0.31 mT) and with the H atoms placed in the semi-quinoidal moiety (a_H = 0.22 mT)(see Section 7 of ESI file, Figures S35 and S36). These results evidence that, even at low temperature, the unpaired electron in both compounds is coupled with the two equivalent N atoms at both extremities of the molecule, in line with a fully delocalized structure or with a class III MV species, as already deduced from the discussion of theoretical and optical data.

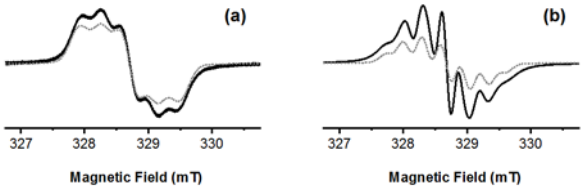

Figure 5. Electron paramagnetic resonance (EPR) spectra of $\mathbf{1}^{\bullet+}$ (a) and $\mathbf{2}^{\bullet-}$ (b) measured at 200 K under nitrogen atmosphere together with their simulated spectra (grey dotted lines). $\mathbf{1}^{\bullet+}$ (g_e = 2.0031, 0.10 mM in DCM) was obtained by oxidation of a solution of **1** with 1 equiv of NO·SbF_6. In the case of $\mathbf{2}^{\bullet-}$ (g_e = 2.0032, 0.20 mM in THF) the addition of 1 equiv of $CoCp_2$ was used.

In conclusion, it is commonly known that in molecule-based electronic devices, like field effect transistors, the attainment of balanced (similar magnitudes) electron and hole mobilities is highly valuable. Therefore, it seems reasonable that this would be also the case for single molecule-based electronics, by which pondered molecular-wire conductances of holes and electrons are highly welcome. This approach is rather new in the field due, in part, to the non-compatibility of a same redox-active organic being simultaneously good electron-donor and -acceptor and a same π–conjugated bridge to be "indifferent" in response to the delocalization of holes or electrons. Here, we have designed and probed the latter case, by preparing mixed valence systems of radical cation and radical anion of perylene-based aromatic and quinoidal bis(diarylamino) and bis(arylimine) bridges. The framework of the Marcus-Hush theory has been used to extract the relevant parameters (i.e., the electronic coupling) that allows us to conclude about the performance/efficiency of the resonance of the charge in the bridge between external groups A complete study by electrochemistry, optical spectroscopy, EPR spectroscopy and quantum chemical calculations has been carried out. This work contributes to the knowledge of molecule-based designs and structure-function relationships that might help the development of the molecular-based electronic, the last link of the highest miniaturization in electronics.

ASSOCIATED CONTENT

Supporting Information

The Supporting Information is available free of charge on the ACS Publications website.

AUTHOR INFORMATION

Corresponding Author

casado@uma.es (J.C.); fabrizia.negri@unibo.it (F.N.); chmwuj@nus.edu.sg (J.W.)

Notes

The authors declare no competing financial interests.

ACKNOWLEDGMENT

The authors are grateful for the financial support received from: MOTHER (MAT2016-80826-R) granted by the DGI (Spain), Gen-Cat (2017-SGR-918) financed by DGR (Catalunya) and the Spanish Ministry of Economy and Competitiveness, through the "Severo Ochoa" Programme for Centres of Excellence in R&D (SEV-2015-0496) and through the project reference CTQ2015-69391. P. P. M. B. gratefully acknowledges financial support from the Juan de la Cierva-Formación 2015 programme (FJCI-2015-23577) supported by MINECO and DAAD through the Research Grants- Short-Term Grants, 2017 programme (No: 91673720). J. W. thanks financial support from Ministry of Education Tier 3 program (MOE2014-T3-1-004).

REFERENCES

1. Hankache, J.; Wenger, O. Organic Mixed Valence, *Chem. Rev.* **2011**, *111*, 5138–5178.

2. Brunschwig B. S.; Sutin , N. Energy Surfaces, Reorganization Energies, and Coupling Elements in Electron Transfer. *Coord. Chem. Rev.* **1999**, *187*, 233–254.

3. Robin, M. D.; Day, P. Mixed-Valence Chemistry: A Survey and Classification. *Adv. Inorg. Radiochem.* **1967**, *10*, 247–422.

4. Hush, N. S. Distance Dependence of Electron Transfer Rates. *Coord. Chem. Rev.* **1985**, *64*, 135–157.

5. Launay, J.-P. Long-distance Intervalence Electron Transfer. *Chem. Soc. Rev.* **2001**, *30*, 386–397.

6. Heckmann, A.; Lambert, C. Organic Mixed-valence Compounds: A Playground for Electrons and Holes. *Angew. Chem. Int. Ed.* **2012**, *51*, 326–392.

7. Richardson, D.E.; Taube, H. Electronic Interactions in Mixed-valence Molecules as Mediated by Organic Bridging Groups. J. *Am. Chem. Soc.***1983**, *105*, 40–51.

8. Nelsen, S. F. Almost Delocalized Intervalence Compounds. *Chem. Eur. J.* **2000**, *6*, 581–588.

9. Barlow, S.; Risko, C.; Odom, S. A.; Zheng, S.; Coropceanu, V.; Beverina, L.; Brédas, J. L.; Marder, S. R. Tuning Delocalization in the Radical Cations of 1,4-Bis[4-(diaylamino)styryl]benzenes, 2,5-Bis[4-(diarylamino)styryl]thiophenes, and 2,5-Bis[4-(diarylamino)styryl]pyrroles Through Substutuent Effects. *J. Am. Chem. Soc.* **2012**, *134*, 10146–10155.

10. Kaafarani, B. R.; Risko, C.; El-Assaad, T. H.; El-Ballouli, A. O.; Marder, S. R.; Barlow, S. Mixed-Valence Cations of Di(carbazol-9-yl) Biphenyl, Tetrahydropyrene, and Pyrene Derivatives, *J. Phys. Chem. C* **2016**, *120*, 3156–3166.

11. Hansmann, M. M.; Melaini, M.; Bertrand, G. Organic Mixed Valence Compounds Derived From Cyclic (alkyl)(amino)carbenes, *J. Am. Chem. Soc.* **2018**, *140*, 2206−2213.

12. Mayorga Burrezo, P.; Lin, N.-T.; Nakabayashi, K.; Ohkoshi, S.-i.; Calzado, E. M.; Boj, P. G.; Díaz García, M. A.; Franco, C.; Rovira, C.; Veciana, J.; Moos, M.; Lambert, C.; López Navarrete, J. T.; Tsuji, H.; Nakamura, E.; Casado J. Bis(aminoaryl) Carbon-Bridged Oligo(phenylenevinylene)s Expand the Limits of Electronic Couplings. *Angew. Chem. Int. Ed.* **2017**, *56*, 2898–2902.

13. Pappenfus, T. M.; Raff, J. D.; Hukkanen, E. J.; Burney, J. R.; Casado, J.; Drew, S. M.; Miller, L. L.; Mann, K. R. Dinitro and Quinodimethane Derivatives of Terthiophene That Can Be Both Oxidized and Reduced. Crystal Structures, Spectra, and a Method for Analyzing Quinoid Contributions to Structure. *J. Am. Chem. Soc.* **2002**, *67*, 6015–6024.

14. Casado, J.; Zgierski, M. Z.; Ewbank, P.C.; Burand, M. W.; Janzen, D. E.; Mann, K. R.; Pappenfus, T. M.; Berlin, A.; Pérez-Inestrosa, E.; Ponce Ortiz, R.; López Navarrete, J. T. Exploration of Ground and Excited Electronic States of Aromatic and Quinoid *S,S*-Dioxide Terthiophenes. Complementary Systems for Enhanced Electronic Organic Materials, *J. Am. Chem. Soc.* **2006**, *128*, 10134–10144

15. Mayorga Burrezo, P.; Zafra, J. L.; López Navarrete, J. T.; Casado J. Quinoidal/aromatic Transformations in π-Conjugated Oligomers: Vibrational Raman Studies on the Limits of Rupture of π-Bonds, *Angew. Chem. Int. Ed.* **2017**, *56*, 2250–2259.

16. Zeng, Z.; Ishida, M.; Zafra, J. L.; Zhu, X.; Sung, Y. M.; Bao, N.; Webster, R. D.; Lee, B. S.; Li, R.-W.; Zeng, W.; Li, Y.; Chi, C.; López Navarrete, J. T.; Ding, J.; Casado, J.; Kim, D.; Wu, J. Pushing Extended *p*-Quinodimethanes to the Limit: Stable Tetracyano-oligo(*N*-annulated perylene)quinodimethanes with Tunable Ground States, *J. Am. Chem. Soc.* **2013**, *135*, 6363–6371.

17. Zeng, Z.; Lee, S.; Zafra, J. L.; Ishida, M.; Zhu, X.; Sun, Z.; Ni, Y.; Webster, R. D.; Li, R.-W.; López Navarrete, J. T.; Chi, C.; Ding, J.; Casado, J.; Kim, D.; Wu, J. Tetracyanoquaterrylene and

Tetracyanohexarylenequinodimethanes with Tunable Ground States and Strong Near-infrared Absorption, *Angew. Chem. Int. Ed.* 2**013**, *52*, 8561–8565.

18. Zeng, W.; Hong, Y.; Medina Rivero, S.; Kim, J.; Zafra, J. L.; Phan, H.; Gopalakrishna, T. Y.; Herng, T. S.; Ding, J.; Casado, J.; Kim, D.; Wu, J. Stable Nitrogen-centered Bis(imino)rylene Diradicaloids. *Chem. Eur. J.* **2018**, *24*, 4944–4951.

19. Jiang, W.; Xiao, C.; Hao, L.; Wang, Z.; Ceymann, H.; Lambert, C.; Di Motta, S.; Negri, F. Localization/Delocalization of Charges in Bay-Linked Perylene Bisimides. *Chem. Eur. J.* **2012**, *18*, 6764 – 6775.

20. Coropceanu, V.; Gruhn, N. E.; Barlow, S.; Lambert, C.; Durivage, J. C.; Bill, T. G.; Nöll, G.; Marder, S. R.; Brédas, J. L. Electronic Couplings in Organic Mixed-valence Compounds: The Contribution of Photoelectron Spectroscopy. *J. Am. Chem. Soc.* **2004**, *126*, 2727–2731.

21. Lambert, C.; Nöll, G. The Class II/III Transition in Triarylamine Redox Systems. *J. Am. Chem. Soc.* **1999**, *121*, 8434–8442.

22. Nelsen, S. F.; Konradsson, A. E.; Weaver, M.N.; Telo, J.P. Intervalence Near-IR spectra of Delocalized Dinitroaromatic Radical Anions, *J. Am. Chem. Soc.* **2003**, *125*, 12493–12501.

23. Nelsen, S. F.; Weaver, M. N.; Zink, J. I.; Telo, J. P. Optical Spectra of Delocalized Dinitroaromatic Radical Anions Revisited. *J. Am. Chem. Soc.* **2005**, *127*, 10611–10622.

24. Rodríguez González, S.; Caballero, R.; Dela Cruz, P.; Langa, F.; López Navarrete, J.T.; Casado, J. Delocalzation-to-localization Charge Transfer Transition in Diferrocenyl-oligothiophenevinylene Molecular Wires as a Function of the Size by Raman Spectroscopy. *J. Am. Chem. Soc.* **2012**, *134*, *134*, 5675–5681.

25. Li, Y.; Chandra Mondal, K.; Samuel, P. P.; Zhu, H.; Orben, C. M.; Panneerselvam, S.; Dittrich, B.; Schwederski, B.; Kaim, W.; Modal, T.; Koley, D.; Roesky, H. W. C4 Cumulene and The Corresponding Air-stable Radical Cation and Dication. *Angew. Chem. Int. Ed.* **2014**, *53*, 4168–4172.

SYNOPSIS TOC (Word Style "SN_Synopsis_TOC"). If you are submitting your paper to a journal that requires a synopsis graphic and/or synopsis paragraph, see the Instructions for Authors on the journal's homepage for a description of what needs to be provided and for the size requirements of the artwork.